

Figure S1| Characterization of RBCEVs, mouse lung epithelial cells and α -EGFR-VHH binding affinity

(A) Western blot of ALIX, TSG101, GPA, HBA, β -actin and GAPDH in RBCs and RBCEVs. **(B)** Single-EV flow cytometry analysis of GPA in RBCEVs with a gating strategy to obtain a distinct population of RBCEVs from the background noise. **(C)** Flow cytometry analysis of EpCAM expression in mouse lung epithelial cells and α -EGFR-VHH binding affinity to multiple cells.

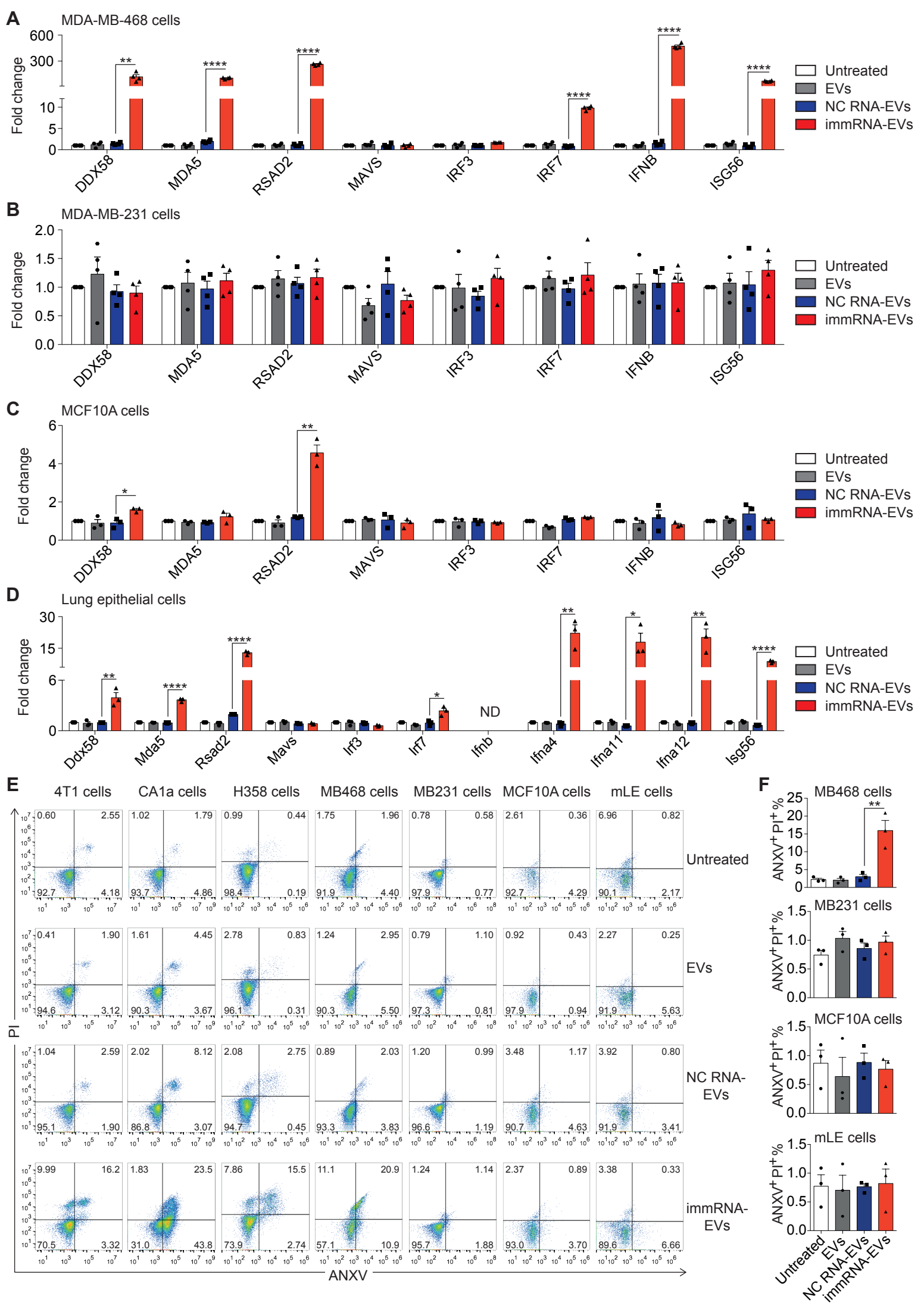


Figure S2| The effects of immRNA-loaded RBCEVs on cancer cells and non-malignant cells

(A-D) qPCR analysis of *DDX58* and its downstream effectors relative to *GAPDH* in MDA-MB-468 (A), MDA-MB-231 (B), MCF10A (C) and mouse lung epithelial cells (D) treated with 0.1 $\mu\text{g}/\mu\text{L}$ unloaded or NC-RNA-loaded, immRNA-loaded RBCEVs for 24 hours (n = 3-4, RNA loaded using REG1) ND, not detected. **(E)** Representative flow cytometric plots of ANXV/PI staining in 4T1, CA1a, H358, MDA-MB-468 (MB468), MDA-MB-231 (MB231), MCF10A and mouse lung epithelial (mLE) cells treated with 0.1 $\mu\text{g}/\mu\text{L}$ unloaded RBCEVs, NC RNA-loaded RBCEVs and immRNA-loaded RBCEVs for 72 hours. **(F)** Average percentage of ANXV⁺PI⁺ population in MB468, MB231, MCF10A and mLE cells treated with RBCEVs as in (E) (n = 3). All bar graphs represent mean \pm SEM. **P* < 0.05, ***P* < 0.01 and *****P* < 0.0001 determined by Student's two-tailed *t*-test.

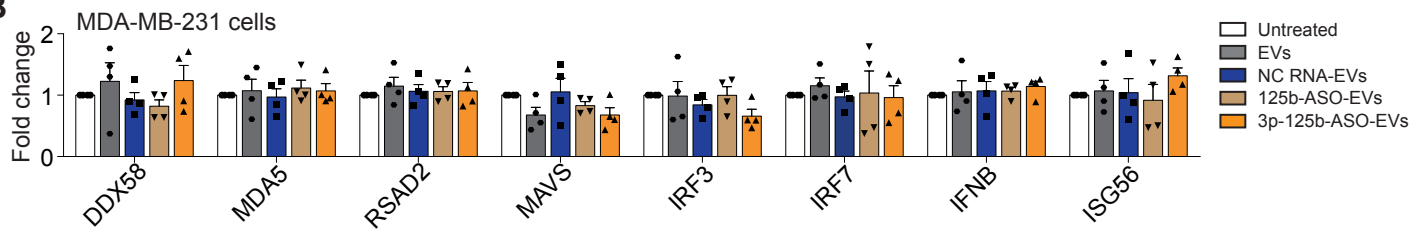
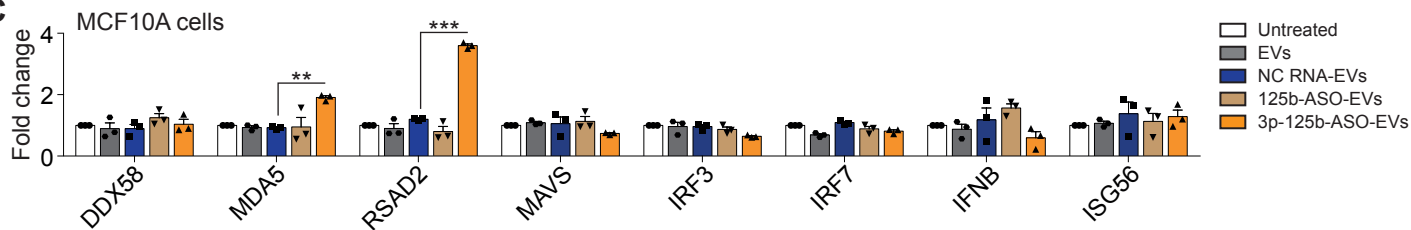
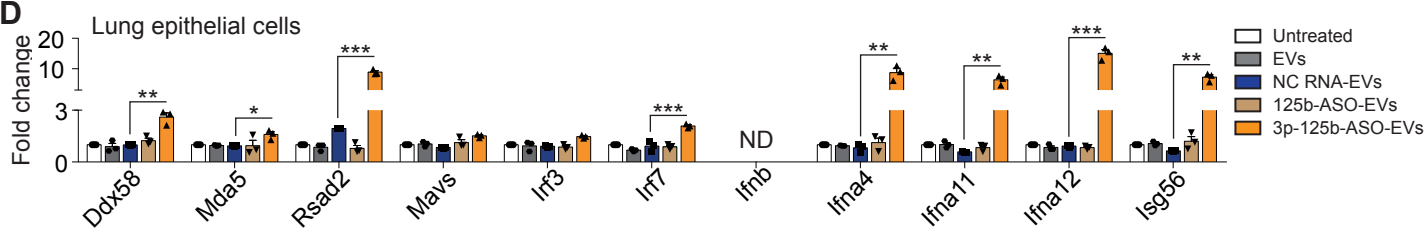
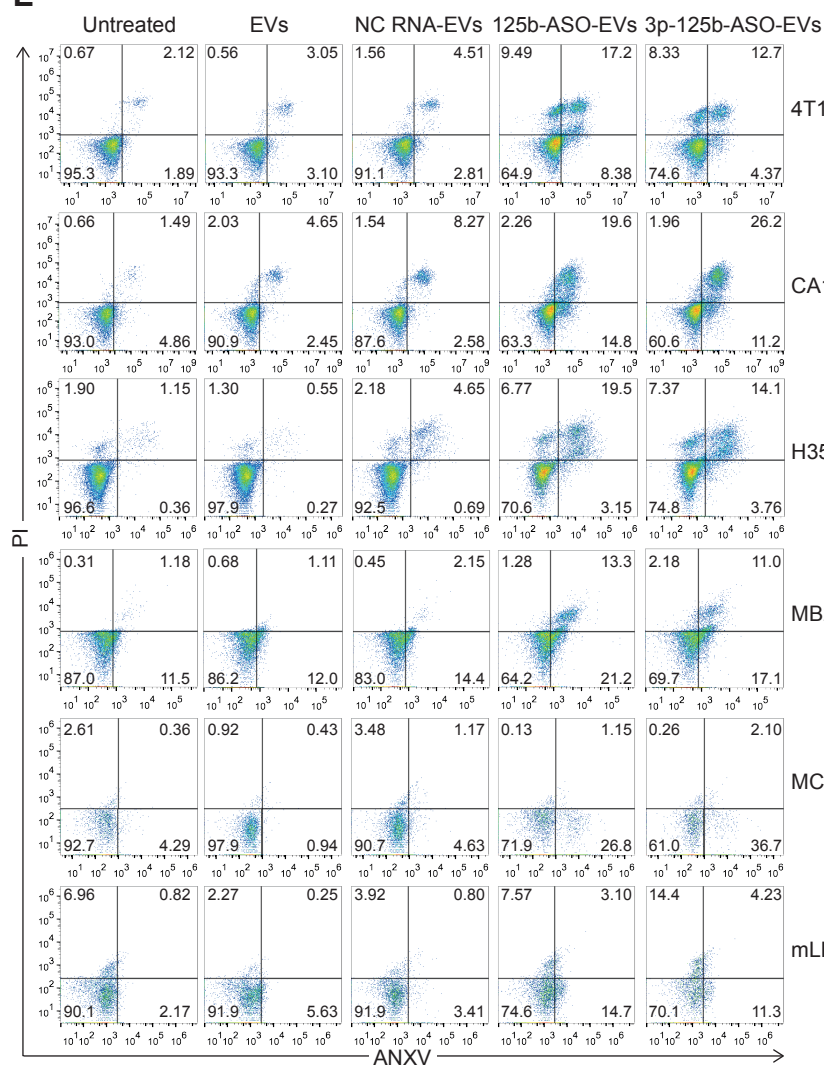
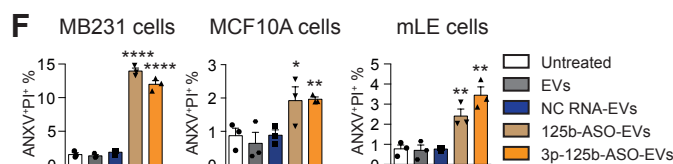
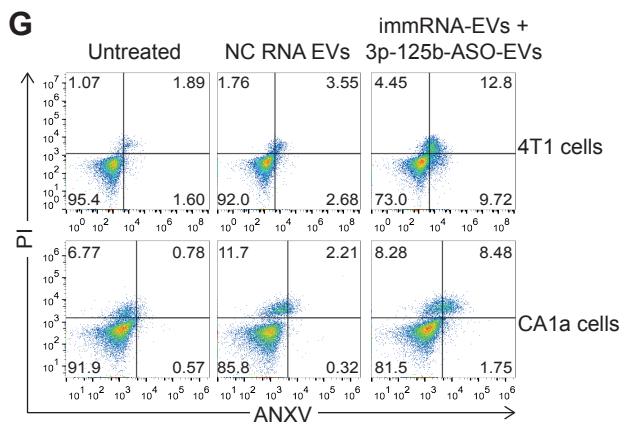
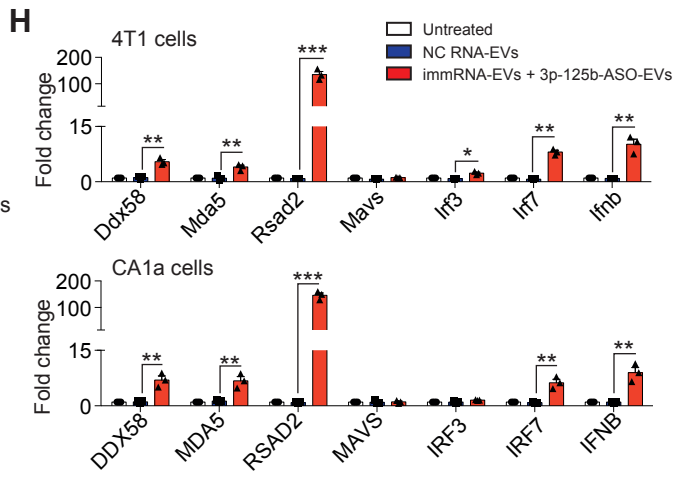
A**B****C****D****E****F****G****H**

Figure S3| The effects of 3p-125b-ASO-loaded RBCEVs on cancer cells and non-malignant cells

(A) Secondary structure of 3p-125b-ASO. **(B-D)** qPCR analysis of *DDX58* and its downstream effectors relative to *GAPDH* in MDA-MB-231 (B), MCF10A (C) and mouse lung epithelial cells (D) treated with 0.1 $\mu\text{g}/\mu\text{L}$ unloaded or NC-RNA-loaded, 125b-ASO-loaded and 3p-125b-ASO-loaded RBCEVs for 24 hours (n = 3-4, RNA loaded using REG1) ND, not detected. **(E)** Representative flow cytometric plots of ANXV/PI staining in 4T1, CA1a, H358, MDA-MB-231 (MB231), MCF10A and mouse lung epithelial (mLE) cells treated with 0.1 $\mu\text{g}/\mu\text{L}$ unloaded or NC RNA-loaded, 125b-ASO-loaded and 3p-125b-ASO-loaded RBCEVs for 72 hours. **(F)** Average percentage of ANXV⁺PI⁺ population in MB231, MCF10A and mLE cells treated with RBCEVs as in (E) (n = 3). **(G)** Representative flow cytometric plots of ANXV/PI staining in 4T1 cells and CA1a cells after a treatment with combined 3p-125-ASO- and immRNA-loaded RBCEVs for 72 hours. **(H)** qPCR analysis of RIG-I pathway gene expression in 4T1 cells and CA1a cells after a treatment with combined 3p-125-ASO- and immRNA-loaded RBCEVs for 24 hours. All bar graphs represent mean \pm SEM. **P* < 0.05, ***P* < 0.01, ****P* < 0.001 and *****P* < 0.0001 determined by Student's two-tailed *t*-test.

A Example of flow cytometric analysis

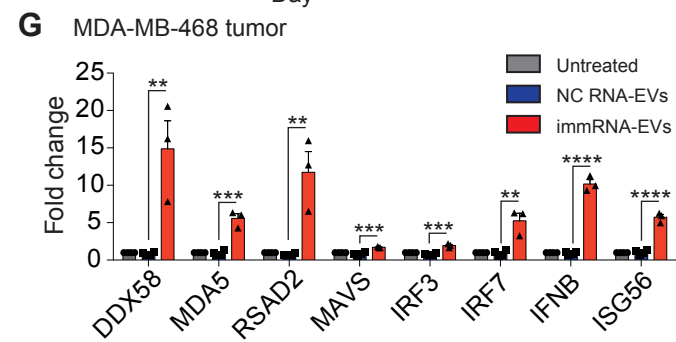
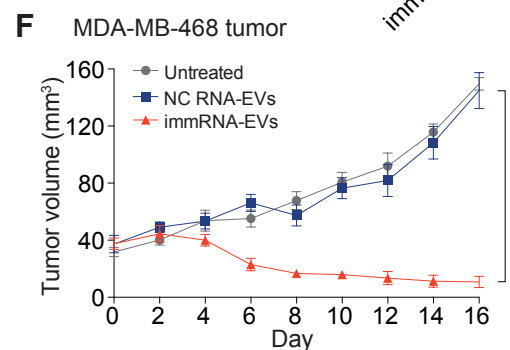
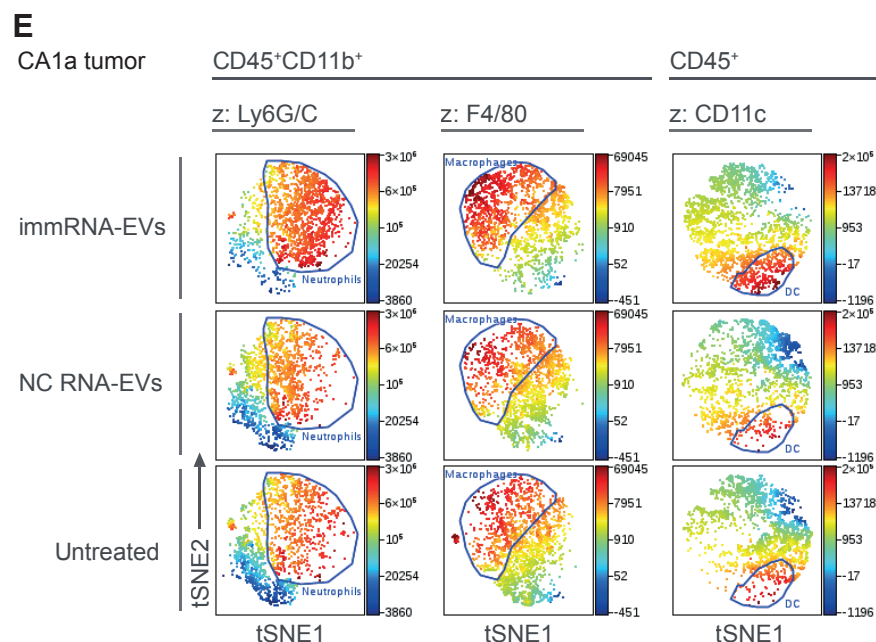
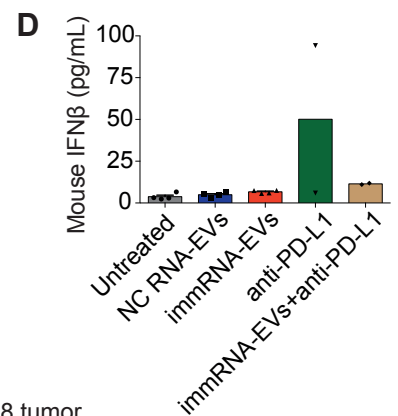
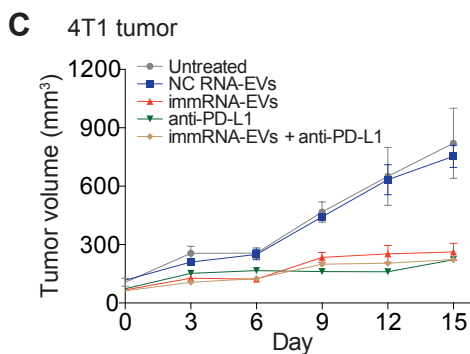
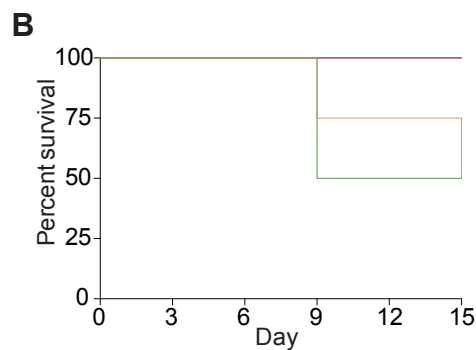
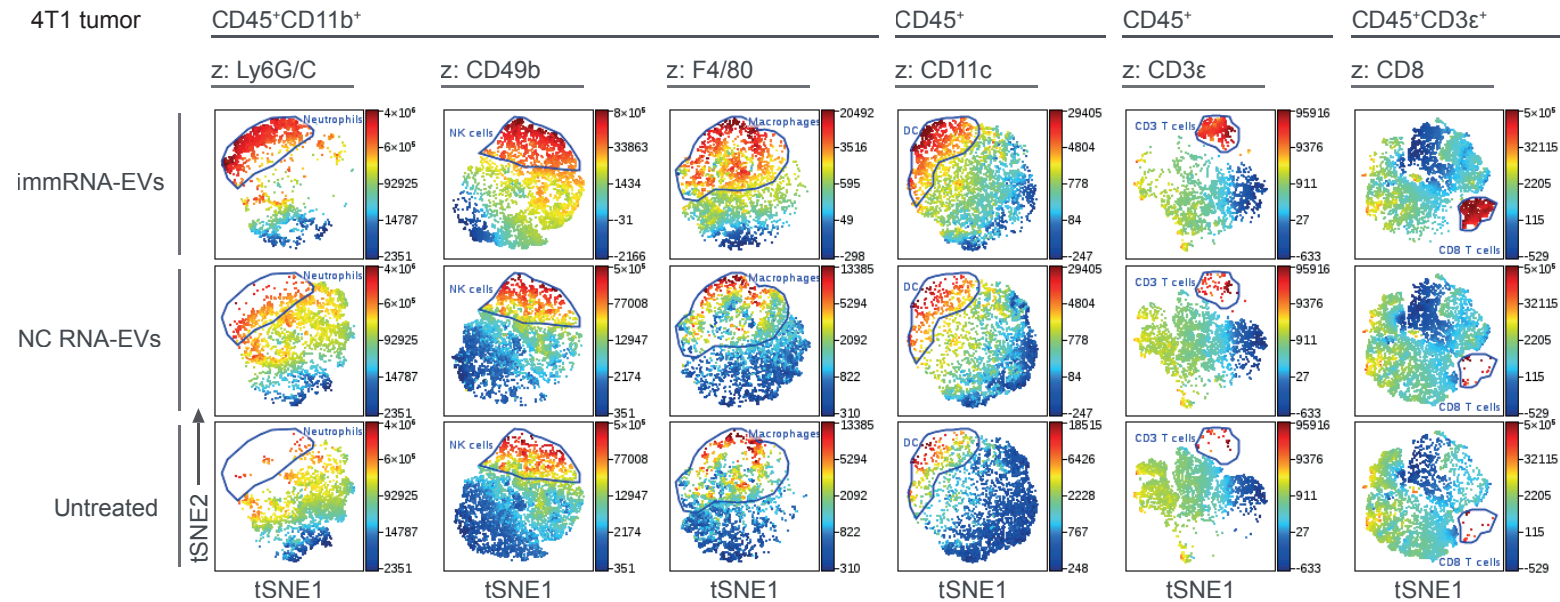
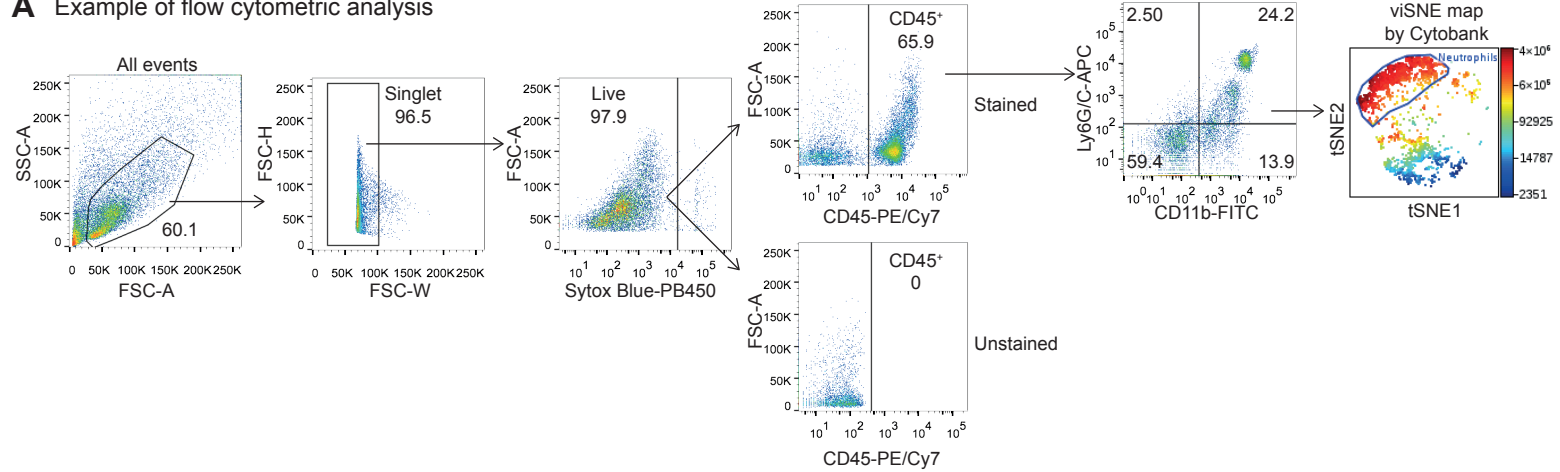


Figure S4| Therapeutic efficacy of immRNA-loaded RBCEVs in mammary tumors

(A) Flow cytometry analysis of immune cells in 4T1 mammary tumors treated with immRNA-loaded RBCEVs as in Figure 4. Cells were gated based on FSC-A and SSC-A to exclude the debris and dead cells. The single cells were further gated based on FSC-W and FSC-H to exclude doublets and aggregates. The live cells were gated from singlet population based on SytoxTM Blue negative. Subsequently, the fluorescence of phenotypic markers for immune cells were gated based on the fluorescent channels and subjected to viSNE analysis. **(B)** Survival of mice with orthotopic 4T1 tumors treated with 2.5 mg/kg NC-RNA-RBCEVs (i.t.), 2.5 mg/kg immRNA-RBCEVs (i.t.), 2 mg/kg anti-PD-L1 antibody (i.p.) as well as 2.5 mg/kg immRNA-RBCEVs (i.t.) in combination with 2 mg/kg anti-PD-L1 antibody (i.p.) (n = 2-4 mice). **(C)** Tumor growth of mice treated as in (B) (n = 2-4 mice). **(D)** ELISA quantification of IFN β in the sera of mice bearing 4T1 tumors treated as in (B) (n = 2-4 mice). **(E)** Representative viSNE plots of immune cells in CA1a mammary tumors treated with immRNA-loaded RBCEVs as in Figure 4. **(F)** Volume of MDA-MB-468 tumors injected intratumorally with 2.5 mg/kg RBCEVs containing immRNA or NC RNA every three days (n = 3-4 mice). **(G)** qPCR analysis of the RIG-I pathway gene expression relative to *GAPDH* in untreated and treated MDA-MB-468 tumors (n = 3-4 mice). All bar graphs represent mean \pm SEM. ** $P < 0.01$, *** $P < 0.001$ and **** $P < 0.0001$ determined by Student's two-tailed *t*-test.

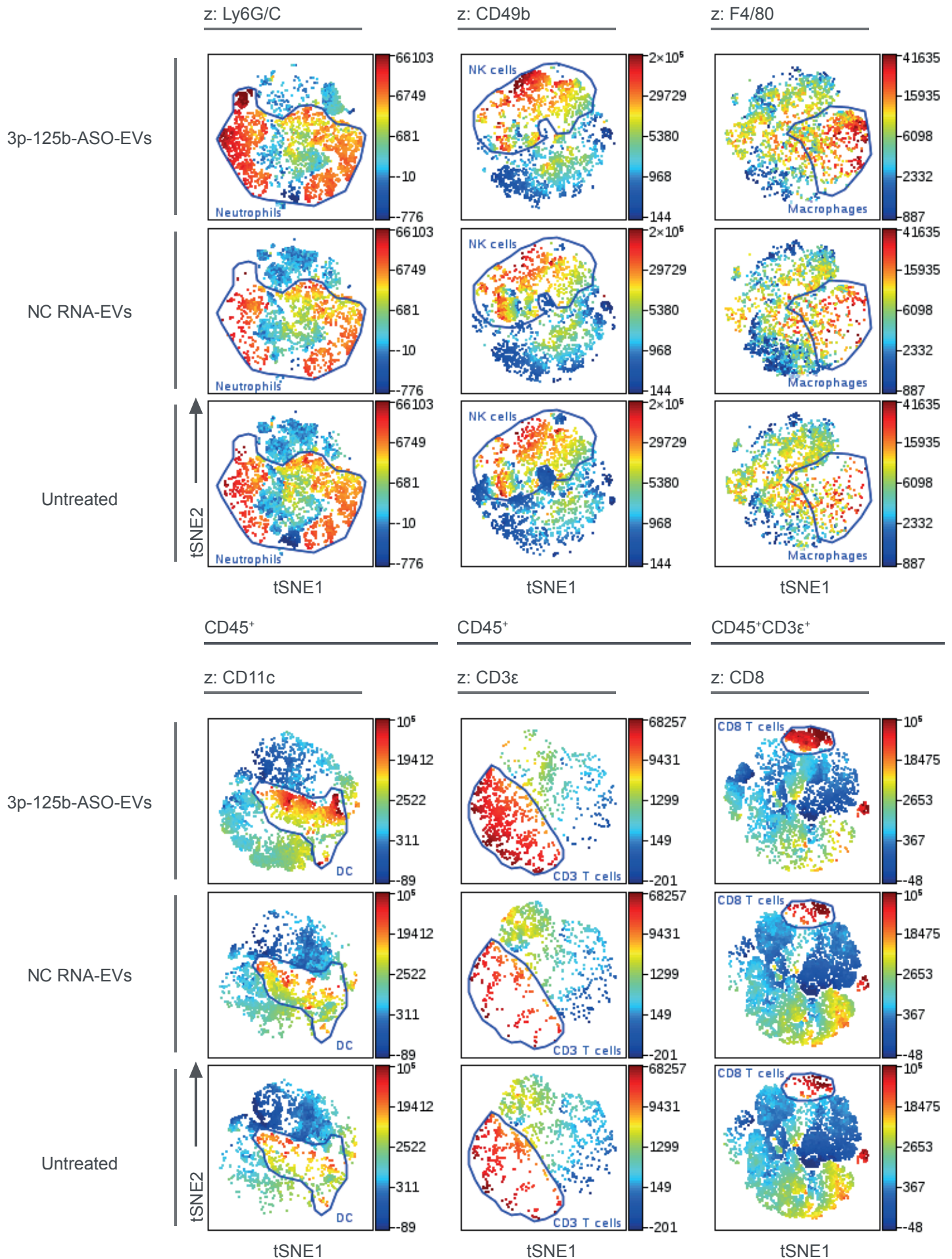


Figure S5| Flow cytometry analysis of immune cells in 4T1 mammary tumors treated with 3p-125b-ASO-loaded RBCEVs. Representative viSNE plots of immune cells in 4T1 mammary tumors treated with 3p-125b-ASO-loaded RBCEVs.

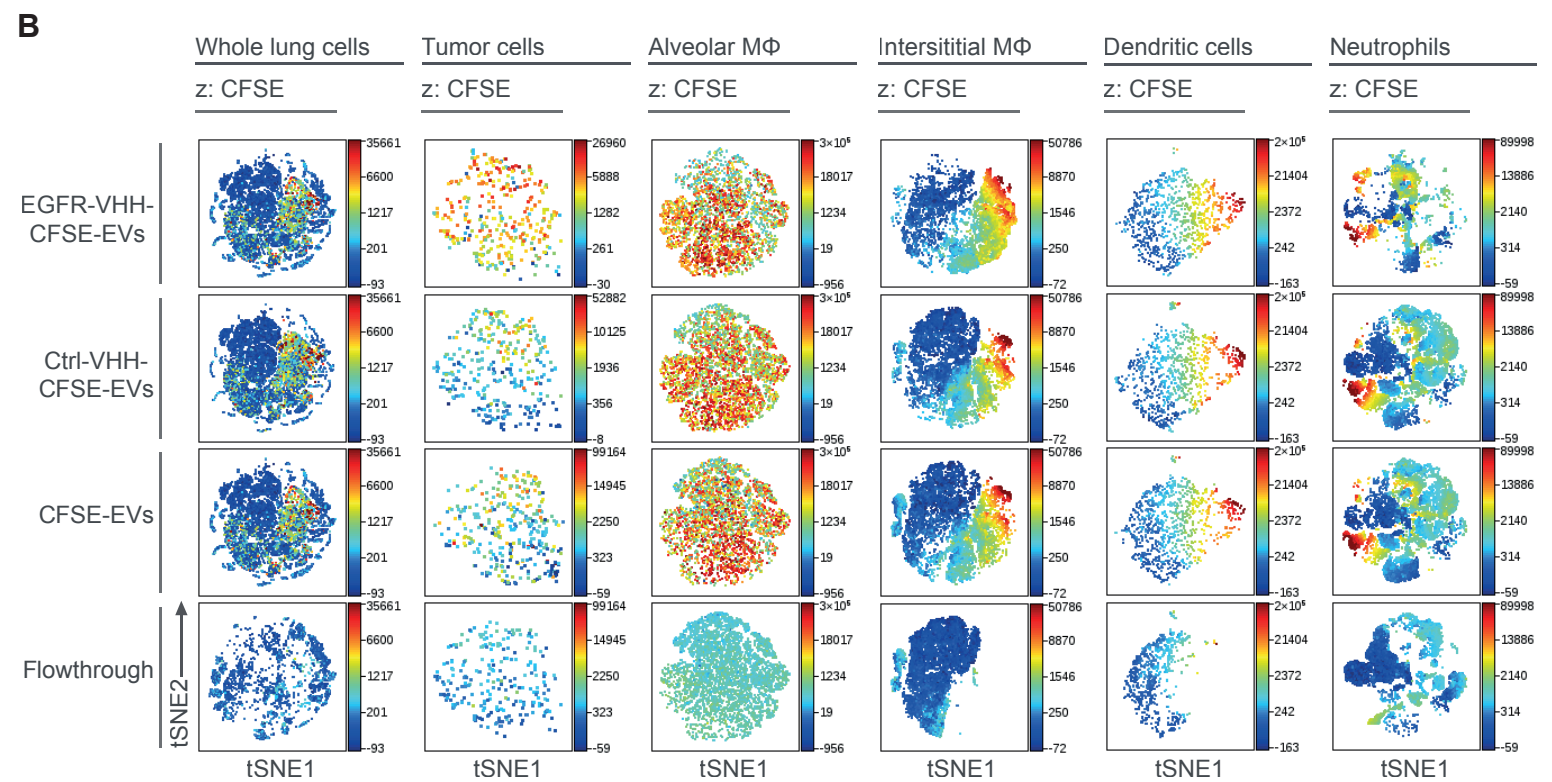
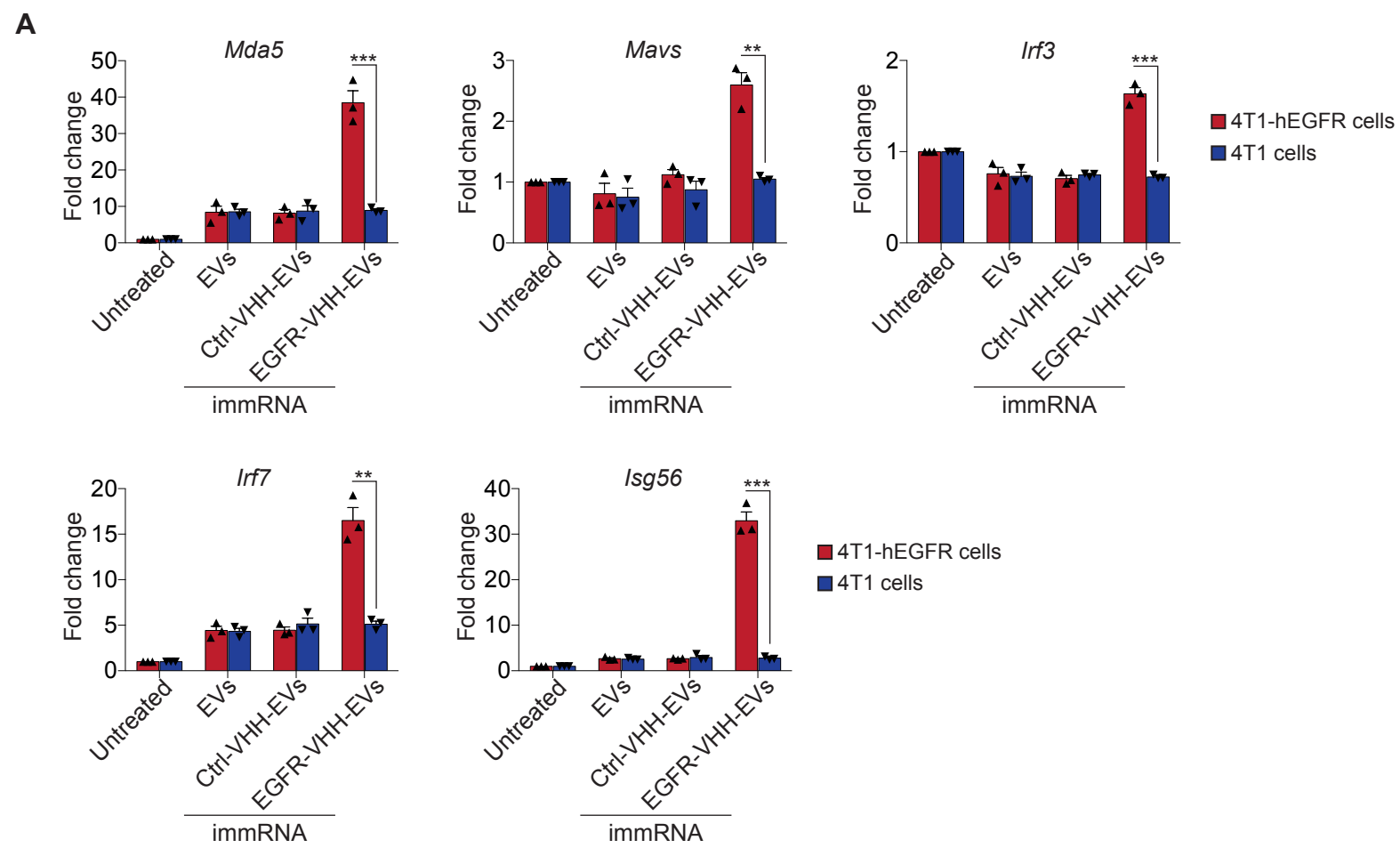


Figure S6| EGFR-VHH-RBCEVs target 4T1-hEGFR cells *in vitro* and 4T1-hEGFR lung metastatic tumors *in vivo*
(A) qPCR analysis of the RIG-I pathway gene expression relative to *Gapdh* in 4T1-hEGFR cells and parental 4T1 cells treated with 0.1 $\mu\text{g}/\mu\text{L}$ uncoated, Ctrl-VHH-coated and EGFR-VHH-coated RBCEVs containing immRNA ($n = 3$). All bar graphs represent mean \pm SEM. ** $P < 0.01$ and *** $P < 0.001$ determined by Student's two-tailed *t*-test. **(B)** Representative viSNE plots of biodistribution of EGFR-VHH-coated CFSE-RBCEVs in respective cell type in the lungs with 4T1-hEGFR metastatic tumors.

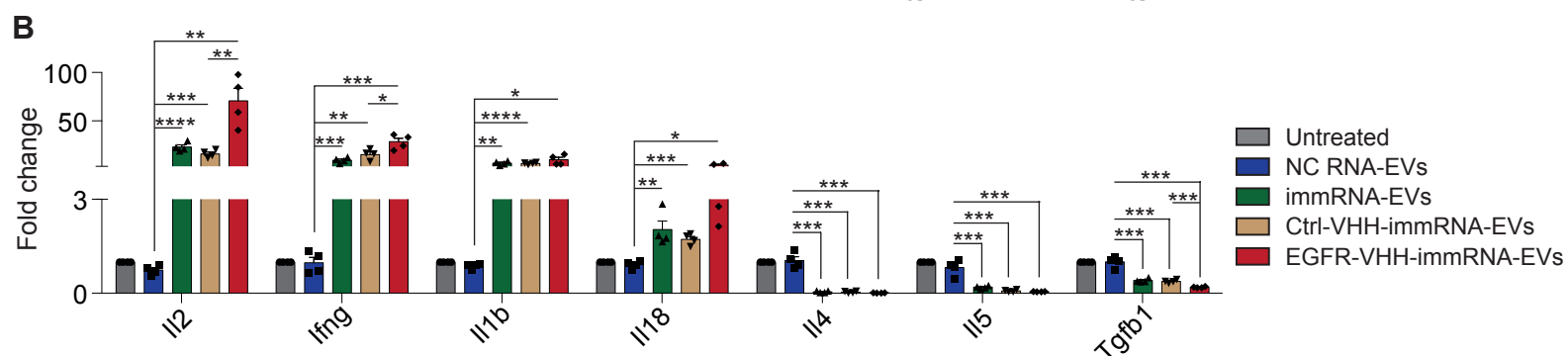
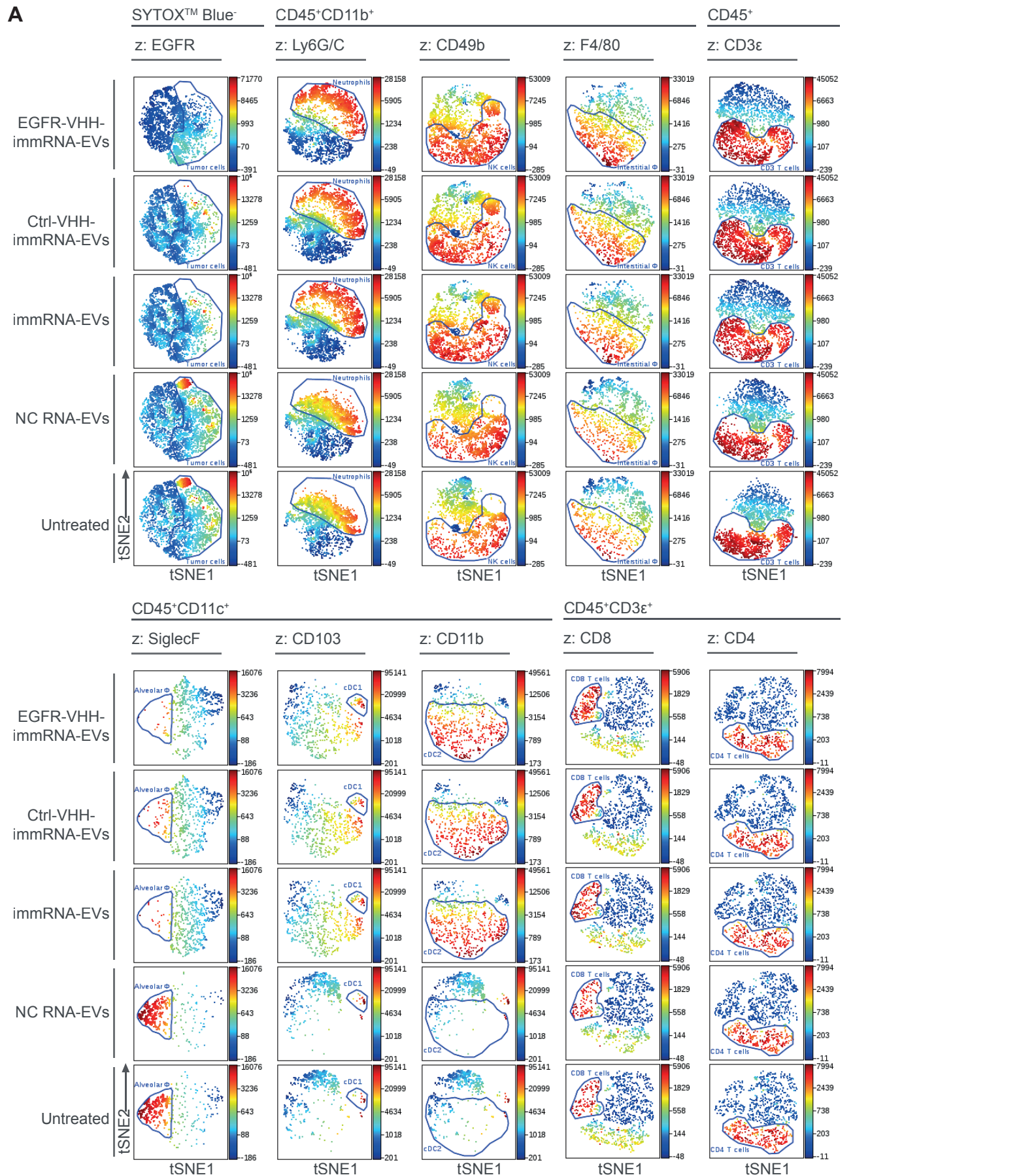


Figure S7| Flow cytometry analysis of immune cells in the lungs with 4T1 metastatic tumors treated with EGFR-VHH-immRNA-RBCEVs

(A) Representative viSNE plots of respective cell type in the lungs with 4T1 metastatic tumors treated with EGFR-VHH-immRNA-RBCEVs. **(B)** qPCR analysis of cytokine gene expression relative to *Gapdh* in the lungs of mice with 4T1-hEGFR metastatic tumors (n = 4 mice). All bar graphs represent mean \pm SEM. * $P < 0.05$, ** $P < 0.01$, *** $P < 0.001$ and **** $P < 0.0001$ determined by Student's two-tailed *t*-test.

Table S1| List of primers

Genes	F/R	Mouse	Human
<i>GAPDH</i>	F R	AGGTCGGTGTGAACGGATTTG TG TAG ACC AT GT AG TT G AG GT CA	GGAGCGAGATCCCTCCAAAAT GGCTGTTGTCATACTTCTCATGG
<i>DDX58</i>	F R	GAG AGT CAC GGG ACC CAC T CGG TCT TAG CAT CTC CAA CG	GCCATTACACTGTGCTTGGAGA CCAGTTGCAATATCCTCCACCA
<i>MDA5</i>	F R	TGATGCACTATTCCAAGAATAAC TCTGTGAGACGAGTTAGCCAAG	GAGCAACTTCTTTCAACCACAG CACTTCCTTCTGCCAACTTG
<i>RSAD2</i>	F R	ACAGCCAAGACATCCTTCGT AAAAGTTGATCTTCTCCAAACCA	CACAAAGAAGTGTCTGCTTGGT AAGCGCATATATTCATCCAGAAT
<i>MAVS</i>	F R	CTGCCTCACAGCTAGTGACC CCGGCGCTGGAGATTATTG	AGGAGACAGATGGAGACACA CAGAACTGGGCAGTACCC
<i>IFNB</i>	F R	AACCTCACCTACAGGGCGGACTT C TCCCACGTCAATCTTCTCTTGC T	CTCTCCTGTTGTGCTTCTCC GTCAAAGTTCATCCTGTCCTTG
<i>IRF3</i>	F R	CGGAAAGAAGTGTGCGGTT TTTTCTGGGAGTGAGGCAG	ACCAGCCGTGGACCAAGAG TACCAAGGCCCTGAGGCAC
<i>IRF7</i>	F R	AGGGCGTTTTATCTTGCG TGGAGCCCAGCATTCTCT	TGGTCCTGGTGAAGCTGGAA GATGTCGTCATAGAGGCTGTTG G
<i>ISG56</i>	F R	TACAGGCTGGAGTGTGCTGAGA CTCCACTTTCAGAGCCTTCGCA	TAGCCAACATGTCCTCACAGAC TCTTCTACCACTGGTTTCATGC
<i>IL4</i>	F R	ATCATCGGCATTTTGAACGAGG GCAGCTCCATGAGAACAATA	
<i>IL5</i>	F R	CTCTGTTGACAAGCAATGAGACG TCTTCAGTATGTCTAGCCCCTG	
<i>IFNG</i>	F R	GCCACGGCACAGTCATTGA TGCTGATGGCCTGATTGTCTT	
<i>IL2</i>	F R	GTGCTCCTTGTC AACAGCG GGGGAGTTTCAGGTTCTGTA	
<i>TGFB1</i>	F R	CTTCAATACGTCAGACATTCGGG GTAACGCCAGGAATTGTTGCTA	
<i>IL1B</i>	F R	GCAACTGTTCTGAACTCAACT ATCTTTTGGGGTCCGTCAACT	
<i>IL18</i>	F R	GACTCTTGCGTCAACTTCAAGG CAGGCTGTCTTTTGTCAACGA	
<i>IL10</i>	F R	AGCCTTATCGGAAATGATCCAGT GGCCTTGTAGACACCTTGGT	
<i>IL6</i>	F R	TCTATACCACTTCACAAGTCGGA TCTATACCACTTCACAAGTCGGA	
<i>IL12B</i>	F R	TGGTTTGCCATCGTTTTGCTG ACAGGTGAGGTTCACTGTTTCT	

<i>TNF</i>	F	CCTGTAGCCCACGTCGTAG
	R	GGGAGTAGACAAGGTACAACCC

<i>IFNA4</i>	F	CTGGTAATGATGAGCTACTACTG
	R	G CCTTCTCCAAGGGGAATCCAA

<i>IFNA11</i>	F	GGTCCTGGCACAATGAGGA
	R	TCCAAGCAGCAGATGAGTCC

<i>IFNA12</i>	F	AAGACTGAGTGAGAAGGAGTGAG
	R	GAGATGCCAGAATTTGAGCAGTG
